Modeling charge transport in quantum dot light emitting devices with NiO and ZnO transport layers and Si quantum dots

Brijesh Kumar, Stephen A. Campbell, and P. Paul Ruden

Citation: J. Appl. Phys. **114**, 044507 (2013); doi: 10.1063/1.4816680
View online: http://dx.doi.org/10.1063/1.4816680
View Table of Contents: http://jap.aip.org/resource/1/JAPIAU/v114/i4
Published by the AIP Publishing LLC.

Modeling charge transport in quantum dot light emitting devices with NiO and ZnO transport layers and Si quantum dots

Brijesh Kumar,[a] Stephen A. Campbell, and P. Paul Ruden
Department of Electrical and Computer Engineering, University of Minnesota, Minneapolis, Minnesota 55455, USA

(Received 4 June 2013; accepted 9 July 2013; published online 29 July 2013)

We propose a model for quantum dot light emitting devices (QD-LEDs), which explores the most important parameters that control their electrical characteristics. The device is divided into a hole transport layer, several quantum dot layers, and an electron transport layer. Conduction and recombination in the central quantum dot region is described by a system of coupled rate equations, and the drift-diffusion approximation is used for the hole and electron transport layers. For NiO/Si-QDs/ZnO devices with suitable design parameter, the current and light output are primarily controlled by the quantum dot layers, specifically, their radiative and non-radiative recombination coefficients. Radiative recombination limits the device current only at sufficiently large bias. © *2013 AIP Publishing LLC*. [http://dx.doi.org/10.1063/1.4816680]

I. INTRODUCTION

Colloidal quantum dots (QDs) are well suited for display technologies because of their tunable band gap and hence wavelength tunable luminescence properties.[1–4] Optimization and other development efforts potentially can be minimized for different colored light emitting diodes (LEDs) because essentially the same structure may be used to create LEDs of various colors. If appropriately chosen, electron and hole transport layers and their contacts need not be varied. The only structural feature that determines the emission wavelength is the size of the QDs. The procedure to prepare the QDs may stay the same (although the conditions need to be varied to create different sizes), the procedure for deposition of the QDs onto the device could stay the same, the electrode deposition could stay the same, and the transport layer deposition could stay the same. Hence, all the design and optimization required for each of these individual device components can be useful for LEDs of different colors.

QD-LEDs were first presented in the form of hybrid organic/inorganic light emitting devices by Colvin *et al.*[5] and were later improved upon by Coe-Sullivan *et al.*[6] For the hybrid devices, the transport layers were fabricated from organic semiconductors and the QDs from inorganic semiconductors. However, organic transport layers suffer from sensitivity to air exposure and stability problems. Hence, inorganic semiconductor transport layers, NiO and ZnO, were developed and used in a device by Caruge *et al.*[7] This work deals with modeling of QD-LEDs with ZnO and NiO transport layers and Si QDs. It can readily be extended to other inorganic transport layers and QDs. The model can also be applied to hybrid QD-LEDs if the appropriate field and carrier density dependences of organic semiconductor mobilities are incorporated.

[a]Author to whom correspondence should be addressed. Electronic mail: brijesh@umn.edu

QDs have been a subject of intense study ever since their discovery by Ekimov and Onushchenko in 1981.[8] Most of the studies concerning transport in quantum dots are related to microscopic single electron transport at extremely low temperatures.[9–12] Relatively few studies deal with charge transport at room temperature, which is the range of primary interest for applications like light emitting or memory devices.[13,14] In this work, a complete model for modeling charge transport in QD-LEDs is proposed. It incorporates charge transport in the bulk, followed by charge transfer into the quantum dot layers and finally, the transfer amongst the various QD-layers and recombination in the QDs.

II. MODEL DESCRIPTION

The schematic device structure for a QD-LED is show in Fig. 1. Fig. 2 shows the corresponding band diagram. The device essentially consists of a number of quantum dot layers sandwiched between two thin transport layers, an electron transport layer (ETL) and a hole transport layer (HTL). The HTL is contacted by an indium tin oxide (ITO), transparent conducting layer, which acts as a hole injector, whereas the ETL is connected to an aluminium cathode, which acts as an electron injector. The device functions as follows. Electrons are injected from the cathode and holes from the anode and they travel through their respective transport layers to the QDs, where they recombine. If the recombination is radiative, photons are emitted. The photon wavelength depends on the QDs and is completely independent of the transport layers.

The device model can be divided into the following parts:

A. Carrier injection from transport layers into the quantum dot layers
B. Transport among the quantum dot layers
C. Recombination in the quantum dots
D. Coupled rate equations
E. Transport in the ETL and HTL
F. Carrier injection from the contacts.

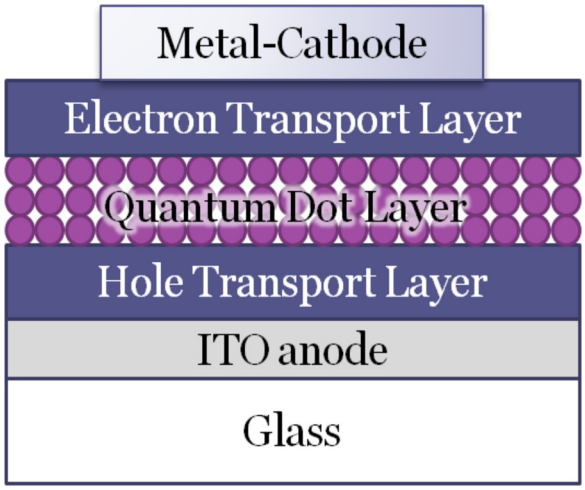

FIG. 1. Schematic device structure for a quantum dot light emitting diode.

Each of the different components of the model is described in Secs. II A–II F.

A. Carrier injection from transport layers into quantum dot layers

Focusing on the QD layer adjacent to the HTL, the quantum dots closest to the HTL are considered to be traps for holes. In equilibrium, using detailed balance, the rate of capture of holes by these QDs is the same as the rate of emission

$$\tilde{e}_0 p_0(0) = \tilde{c}_0 p_0(0^-)\{N_T - p_0(0)\}, \tag{1a}$$

where N_T is the density of trap states in the quantum dot layer (equivalent to the density of quantum dots since each QD can only accommodate one hole), $p(0)$ is the hole density in the quantum dot layer adjacent to the HTL, $p(0^-)$ is the hole density in the HTL very close to the quantum dot layer, $\tilde{e}$ is the emission rate coefficient for the trap states, and $\tilde{c}$ is the capture rate coefficient for the trap states. Whenever a subscript (0) is used it stands for equilibrium.

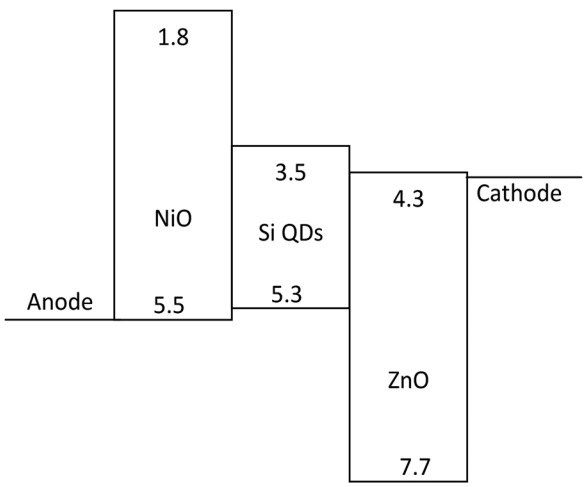

FIG. 2. Flat band diagram for a sample device which consists of Si quantum dots, ZnO as the electron transport layer, NiO as the hole transport layer, and ohmic contacts to both anode and cathode. The horizontal lines at ends signify the metal Fermi energies for anode and cathode. Energies are in eV with respect to the vacuum level.

The ratio of emission and capture coefficients is

$$\frac{\tilde{c}_0}{\tilde{e}_0} = \frac{p_0(0)}{\{N_T - p_0(0)\}p_0(0^-)}. \tag{1b}$$

Under non-equilibrium conditions, the rate of change of carrier concentration is given by the difference of capture and emission, which can be described as

$$\frac{\partial p}{\partial t} = \tilde{c}p(0^-)\{N_T - p(0)\} - \tilde{e}p(0). \tag{1c}$$

If the device is not too far out of equilibrium, the capture and emission coefficients can be taken to be the same as for equilibrium. Furthermore, if the carrier concentration is non-degenerate, Eq. (1c) can be simplified to

$$\frac{\partial p}{\partial t} = \frac{1}{\tau_{pl}}\left\{\frac{p(0^-)}{p_0(0^-)}p_0(0) - p(0)\right\}, \tag{1d}$$

where τ_{pl} $(=1/\tilde{e}_0)$ is capture/emission time constant, a parameter which depends on the materials used. Equations for electrons at the interface between the ETL and the adjacent QD layer are entirely analogous.

B. Transport among the quantum dot layers

The quantum dots can be considered as semiconductor particles with an insulating layer surrounding them.[15] The insulating layer may consist of silicon dioxide[16] or organic ligands,[17] depending on the method used to prepare the quantum dots. The transport from one QD to another is viewed as a direct tunneling process, where the QDs act as potential wells and the insulating layers as tunnel barriers.

Using a one-dimensional WKB approximation, the tunneling probability from QD layer 1→2 can be written as

$$T_{12} = \exp\{-2\kappa(2d_{ins})\}, \tag{2}$$

where kappa is the inverse characteristic length for tunneling and d_{ins} is the thickness of the insulating layer around the QDs.

The electron is "oscillating" in the well with "frequency," $\nu = v_{th}/2d_{Si}$, where v_{th} is the thermal velocity of electrons, d_{Si} is the diameter of the QD, and it has probability T_{12} of making a transition to the neighboring QD layer. The total density of electrons per second tunneling from 1→2 assuming an unoccupied layer 2 is

$$N_{1\to 2} = n_1 \nu T_{12}, \tag{3a}$$

where n_1 is the number of electrons in layer 1.

The "oscillation frequency" is the same for both the layers because the particle size and temperature are the same in layers 1 and 2. Thus, the total number of electrons per second tunneling from 2→1, assuming an unoccupied layer 1, can be written as

$$N_{2\to 1} = n_2 \nu T_{21}. \tag{3b}$$

Consequently, the net flow of electrons from 1→2 is

$$N_{1\to 2} - N_{2\to 1} = \nu(T_{12}n_1 - T_{21}n_2). \tag{3c}$$

By detailed balance, we may write

$$N_{1\to 2} - N_{2\to 1} = w_{12}\left(n_1 - \frac{n_{1o}}{n_{2o}}n_2\right), \tag{3d}$$

where $w_{12} = \nu T_{12} = \frac{v_{th}}{2d_{Si}}\exp\{-2\kappa(2d_{ox})\}$ and n_{1o} and n_{2o} are equilibrium concentrations of electrons in layers 1 and 2, respectively. Similar equations can be written for transport of holes in the QDs.

C. Recombination in the quantum dots

There are two types of recombination in quantum dots, radiative and non-radiative. Radiative recombination can be either monomolecular or bimolecular depending upon the doping of quantum dots. If the quantum dots are doped, then the recombination rate is dependent only on the minority carrier density, hence it is monomolecular. But if the quantum dots are undoped or if both non-equilibrium carrier densities are comparable to the equilibrium carrier density, then the recombination rate depends on both kinds of carriers, i.e., it is bimolecular. In the rest of this work, we assume that the quantum dots are undoped and hence the recombination is bimolecular, as also shown by Kočka *et al.*[18]

Bimolecular recombination rate can be defined as follows:

$$U_r = \gamma(np–{n_i}^2), \tag{4a}$$

where γ is recombination rate coefficient, n and p are electron and hole concentrations, respectively, and n_i is intrinsic carrier concentration.

Non-radiative recombination can be modeled as Shockley-Read-Hall (SRH) recombination[19,20]

$$U_{nr} = \frac{pn - n_i^2}{\tau_n(p + n_1) + \tau_p(n + n_1)}. \tag{4b}$$

Assuming the electron and hole recombination lifetimes to be equal, $\tau_p = \tau_n$ and $p,n \gg n_1$, the total non-radiative recombination rate can be written as

$$U_{nr} = \frac{pn - n_i^2}{\tau_{nr}(p + n)}. \tag{4c}$$

Both radiative and non-radiative recombination take place in parallel in the quantum dots; hence, the total recombination rate can be written as

$$U = U_r + U_{nr} = \gamma(pn - n_i^2) + \frac{pn - n_i^2}{\tau_{nr}(p + n)}. \tag{4d}$$

D. Coupled rate equations

The discretization scheme for the quantum dot layers is shown in Fig. 3. From what has been described in the above subsections, the transport equations for holes can be written in terms of coupled rate equations

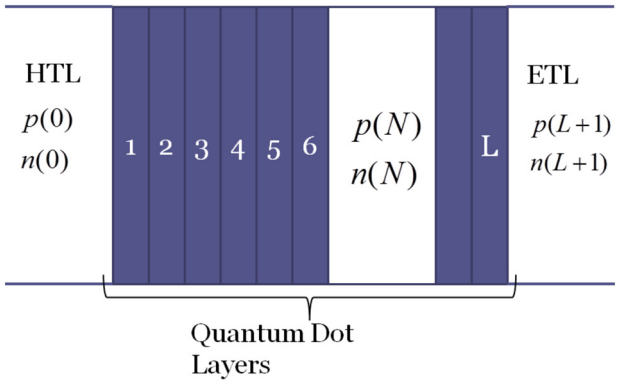

FIG. 3. Discretization scheme for QD-LED focusing on the QD layers.

$$\frac{dp(1)}{dt} = \frac{1}{\tau_{p0,1}}\left\{\frac{p(0)}{p_0(0)}p_0(1) - p(1)\right\} - w_{12}^p\left\{p(1) - \frac{p_0(1)}{p_0(2)}p(2)\right\} - \gamma_1\{n(1)p(1) - n_{i1}^2\} - \frac{p(1)n(1) - n_{i1}^2}{\tau_{nr}(p(1) + n(1))}, \tag{5a}$$

$$\frac{dp(2)}{dt} = w_{12}^p\left\{p(1) - \frac{p_0(1)}{p_0(2)}p(2)\right\} - w_{23}^p\left\{p(2) - \frac{p_0(2)}{p_0(3)}p(3)\right\} - \gamma_2\{n(2)p(2) - n_{i2}^2\} - \frac{p(2)n(2) - n_{i2}^2}{\tau_{nr}(p(2) + n(2))}, \tag{5b}$$

$$\frac{dp(N)}{dt} = w_{N-1,N}^p\left\{p(N-1) - \frac{p_0(N-1)}{p_0(N)}p(N)\right\} - w_{N,N+1}^p\left\{p(N) - \frac{p_0(N)}{p_0(N+1)}p(N+1)\right\} - \gamma_N\{n(N)p(N) - n_{iN}^2\} - \frac{p(N)n(N) - n_{iN}^2}{\tau_{nr}(p(N) + n(N))}, \tag{5c}$$

$$\frac{dp(L)}{dt} = w_{L-1,L}^p\left\{p(L-1) - \frac{p_0(L-1)}{p_0(L)}p(L)\right\} - \frac{1}{\tau_{pL,L+1}}\left\{p(L) - \frac{p(L+1)}{p_0(L+1)}p_0(L)\right\} - \gamma_L\{n(L)p(L) - n_{iL}^2\} - \frac{p(L)n(L) - n_{iL}^2}{\tau_{nr}(p(L) + n(L))}. \tag{5d}$$

The transport equations for electrons can be written in analogous fashion. It is important to note that each of the above equations contain a product of electron and hole densities; thus, we need to employ a solution based on non-linear system of equations.

E. Transport in ETL and HTL

Bulk drift and diffusion is used to describe the transport in the two transport layers. It is represented by the following set of equations:

$$\frac{\partial p}{\partial t} = -\frac{1}{q}\frac{\partial J_p}{\partial x} + G - U, \tag{6a}$$

$$\frac{\partial n}{\partial t} = \frac{1}{q}\frac{\partial J_n}{\partial x} + G - U, \tag{6b}$$

$$\frac{\partial^2 \psi}{\partial x^2} = -\frac{q}{\varepsilon}(N_d - N_a + p - n), \tag{6c}$$

where

$$J_p = -qD_p\frac{\partial p}{\partial x} - qp\mu_p\frac{\partial \psi}{\partial x}, \tag{6d}$$

$$J_n = qD_n\frac{\partial n}{\partial x} - qn\mu_n\frac{\partial \psi}{\partial x}. \tag{6e}$$

Generation is assumed to be negligible and thus neglected from our calculations ($G = 0$). Recombination is assumed to be of Shockley-Read-Hall form[19,20]

$$U = \frac{pn - n_i^2}{\tau_n(p + n_i) + \tau_p(n + n_i)}. \tag{7}$$

F. Carrier injection from the contacts

The contacts at both the anode and cathode are assumed to be ohmic. Thus, the carrier concentrations inside the transport layers, very close to the contacts (positions 0 & w), are equal to the equilibrium carrier concentrations

$$p(0)n(0) = \{n_i(0)\}^2; \quad p(w)n(w) = \{n_i(w)\}^2. \tag{8a}$$

There is no space charge at electrodes,

$$\begin{aligned} N_d(0) - N_a(0) + p(0) - n(0) &= 0; \\ N_d(w) - N_a(w) + p(w) - n(w) &= 0. \end{aligned} \tag{8b}$$

The electrostatic potential at the electrodes is thus given by

$$\begin{aligned} \psi(0) &= V - \frac{kT}{q}\ln\left[\frac{p(0)}{n_i(0)}\right]; \\ \psi(w) &= \frac{kT}{q}\ln\left[\frac{n(w)}{n_i(0)}\right] - \left(\frac{\Delta E_C + \Delta E_V}{2}\right). \end{aligned} \tag{8c}$$

The last term in Eq. (8c) accounts for the discontinuities in the conduction (ΔE_C) and valence (ΔE_V) band, which are estimated from Anderson's rule[21] as described in more detail by Smith.[22] The conduction band and valence band edges of quantum dots do not affect the potential boundary conditions because the electric field in the device is controlled by the difference in the Fermi levels of the transport layers, just like a p-i-n diode, where the electric field in the i-region is controlled by the difference in the Fermi levels of p- and n-regions.

III. RESULTS AND DISCUSSION

A. Device parameters

To illustrate the above described model, the example device structure shown in Fig. 2 is used. A 47 nm thick layer of NiO, which is naturally a p-type, is used as the HTL, while a 50 nm thick ZnO layer, a naturally n-type material, provides the ETL. The emission layer consists of 5 layers of silicon QDs, each 5 nm in diameter including a 0.5 nm thick SiO_2 shell acting as the passivation layer. Thus the total device thickness is 122 nm. The parameters for the transport layers are presented in Table I. The majority carrier mobilities are taken from the literature, but the minority carrier mobilities are not easily available in the literature, so the minority carrier mobilities are assumed to the same as majority carrier mobilities. As demonstrated in Sec. III B, the minority carrier mobility does not matter because the current is dominated by majority carriers. Using the method described by Smith[7,22] and the electron affinity and band gap values given by Caruge *et al.*,[7] the discontinuities in the bands are calculated to be $\Delta E_C = 2.5$ eV and $\Delta E_V = 2.2$ eV. The carrier lifetimes were not available for NiO, so they were assumed to be the same as for ZnO as reported by Liu *et al.*[23]

Table II shows the important parameters relating to the transport in the QD layers. The intrinsic carrier concentration, n_i, is based on the band gap provided by Ligman *et al.*[26] The QDs are assumed to be undoped. The tunneling coefficient is calculated using WKB approximation assuming a 0.5 nm thick oxide shell on the Si QDs. The capture lifetime of an electron/hole by a QD is not easily available in literature. So, the capture lifetimes are varied from 1 ms to 1 ns and the effect of such a change is studied on the device. This is discussed in further detail in Sec. III B. The non-radiative SRH recombination lifetime is assumed to be $\sim$1 μs as observed by Sobolev *et al.*[27]

B. Simulation results

Fig. 4 shows the electron and hole carrier densities and electrostatic potential at equilibrium and for an applied potential of 0.5 V. The built-in potential for the device is 0.98 V as can be seen from Fig. 4. Upon applying the 0.5 V forward bias, the electrostatic potential across the device goes down to 0.48 V as expected. At equilibrium, the carrier

TABLE I. The parameters of NiO and ZnO used for our model device.

	NiO	ZnO
Hole mobility, μp[24]	0.2 cm^2/Vs	8.6 cm^2/Vs
Electron mobility, μn[24,25]	0.2 cm^2/Vs	8.6 cm^2/Vs
Doping concentration	p-type, $N_A = 10^{17}$ cm^{-3}	n-type $N_D = 10^{17}$ cm^{-3}
Bandgap, E_g[7]	3.7 eV	3.4 eV
Intrinsic carrier concentration, n_i	6.106×10^{-13} cm^{-3}	2.0×10^{-10} cm^{-3}
Electron affinity, χ[7]	1.8 eV	4.3 eV
Carrier Lifetime, $\tau_p = \tau_n$[23]	1.2 μs	1.2 μs

TABLE II. The parameters used to describe transport in QD layers.

Intrinsic carrier concentration, n_i	1.42×10^4 cm^{-3}
Tunneling coefficient, w	1.25×10^{10} s^{-1}
Capture lifetime, τ	1×10^{-3} s^{-1} $\times 10^{-9}$ s
Bimolecular Recombination Coefficient, γ[18]	4×10^{-10} cm^3 s^{-1}
Non-radiative recombination lifetime, τ_{nr}[27]	1×10^{-6} s
Band gap, Eg[26]	1.8 eV
Electron affinity, χ[26]	3.5 eV

densities decrease as we move away from the contacts and deeper into the device. Because of the high band gap of the ETL and HTL, only the majority carriers play any significant role in the overall current of the device. As can be seen from Fig. 4, minority carrier densities in both ETL and HTL are more than 20 orders of magnitude lower than the majority carrier densities. In the QD layers, both electron and hole carrier densities are at comparable levels because of the much smaller band gap. When a 0.5 V forward bias is applied, the majority carrier densities in the transport layers increase, both electron and hole densities in the QD layers increase, and as a result, a current of 9.47 μA/cm^2 flows through the device.

The total current density is plotted in Fig. 5 as semilog and linear plots. At low voltages, the current is limited by diffusion, and thus, the current density increases exponentially with increasing forward bias. At high voltages, the current is limited by the series resistance of the device and hence the current increases linearly with forward bias. A semilog plot of the radiative recombination current is also shown in Fig. 5 to compare with the total current. At low voltages, the radiative recombination current is much smaller than the total current, because the SRH recombination dominates over the bimolecular radiative recombination. When a higher forward bias is applied, the carrier densities in the QD increase; thus, the total bimolecular radiative recombination increases (Eq. (4a)). The total SRH recombination (Eq. (4b)) in QDs also increases, but it increases at a lower rate than bimolecular radiative recombination because p and n terms appear both in the numerator and denominator, whereas in bimolecular radiative recombination, they appear only in the numerator. Because of the different rates of increase in the two recombination mechanisms, at around 1 V forward bias, SRH recombination in QDs becomes negligible compared to bimolecular radiative recombination.

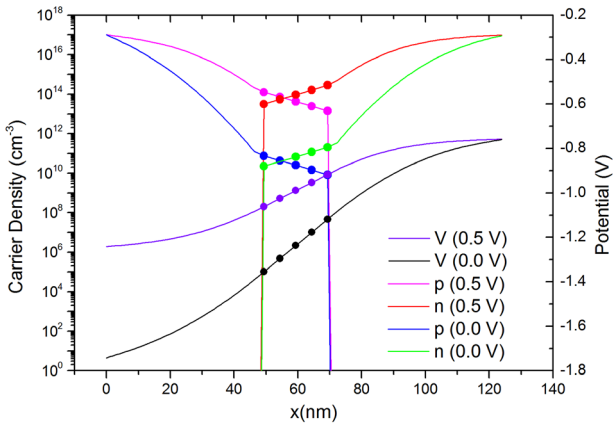

FIG. 4. Carrier densities and electrostatic potential in a device with 5 QD layers (represented by dots on the plot) at equilibrium and with an applied voltage of 0.5 V.

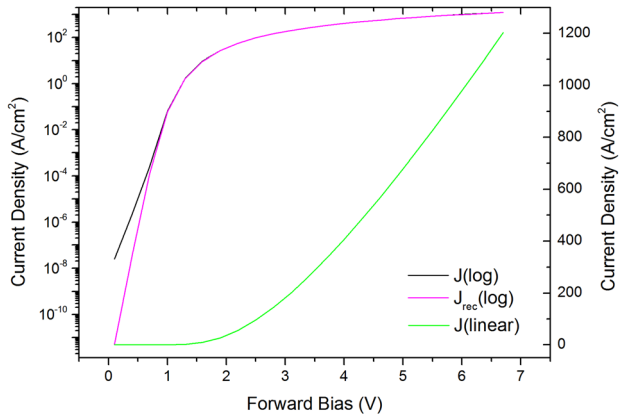

FIG. 5. Total device current density (log and linear) plots with increasing forward bias. The recombination current density is also plotted.

As described in Sec. III A, it is difficult to estimate the capture lifetime, τ, of carriers from the bulk to the quantum dots, so the capture lifetime is varied from 1 ms to 1 ns to assess the effect it has on the device characteristics. Fig. 6 shows the current density vs applied voltage plot for the device with varying carrier capture lifetimes, keeping all others parameters constant. The plots at $\tau = 1$ ns and $\tau = 1$ μs completely overlap each other, and the current density only reduces slightly if $\tau = 1$ ms. Hence, it can be concluded that over a reasonably large range of values, the carrier capture lifetime has negligible effect on the current–voltage characteristics of the device.

We have assumed a radiative recombination coefficient of $\gamma = 4 \times 10^{-10}$ cm^3 s^{-1}. Depending on the fabrication conditions, this coefficient may vary.[28] Thus, we next explore the effect of changing the value of γ. Keeping all the other parameters constant, the effect of the changing γ from 4×10^{-12} cm^3 s^{-1} to 4×10^{-8} cm^3 s^{-1} on current density

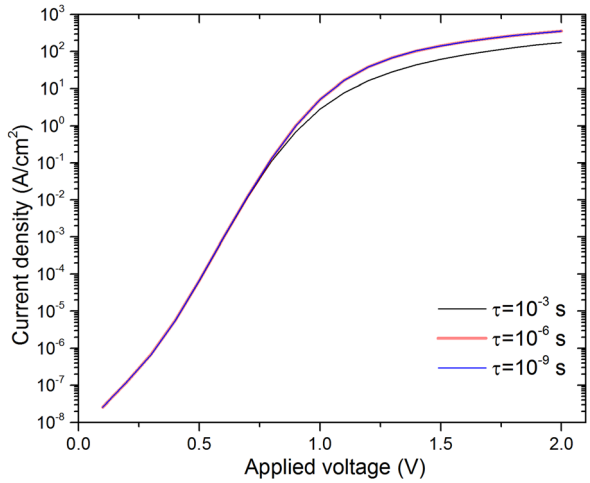

FIG. 6. Current density vs applied voltage for different assumed values of the carrier capture coefficients (τ).

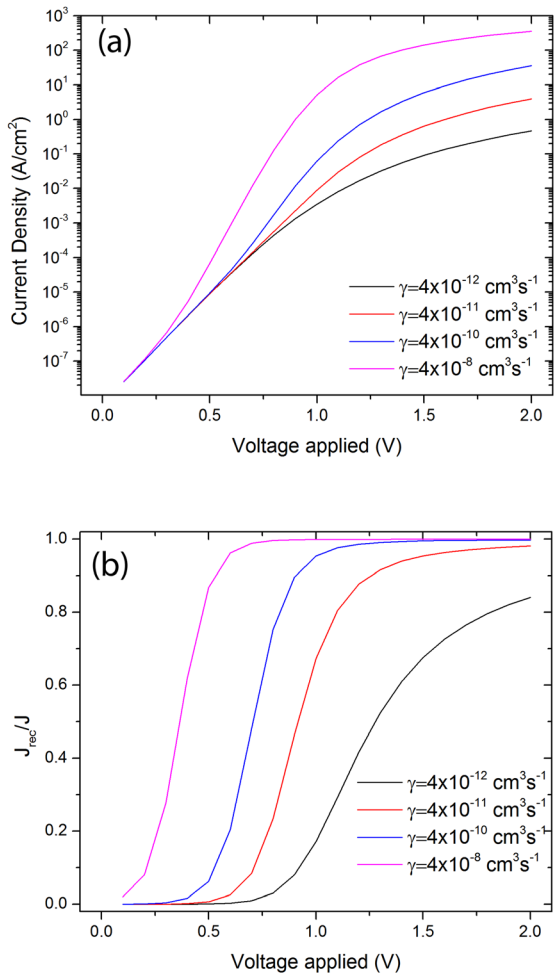

FIG. 7. (a) Current density vs applied voltage and (b) ratio of recombination current to total current (J_{rec}/J) for various radiative recombination coefficients (γ).

and ratio of recombination current to total current is studied and is plotted in Figs. 7(a) and 7(b), respectively. At high forward bias, the total current density increases upon increasing the recombination coefficient, which again indicates that the total current is limited by the radiative recombination current at high forward bias. At low voltages, the total current is limited by the non-radiative recombination current, so the total current density stays nearly constant at voltages below 0.5 V for γ between 4×10^{-12} cm^3 s^{-1} and 4×10^{-10} cm^3 s^{-1}. Both these observations are consistent with our conclusions from Fig. 5 that at low voltages, the current is primarily due to non-radiative recombination and at high voltages, the current is primarily a result of radiative recombination. As observed in Fig. 7(b), the ratio of recombination current to total current increases upon increasing the applied voltage. With increasing γ, the transition point of no recombination current to a positive value of recombination current (the turn on point of the LED) shifts to the left. For γ between 4×10^{-12} cm^3 s^{-1} and 4×10^{-10} cm^3 s^{-1}, the turn-on point is beyond or around 0.5 V forward bias. But, for $\gamma = 4 \times 10^{-8}$ cm^3 s^{-1}, the turn-on point is at almost 0 V. Thus, the current density plot corresponding to for $\gamma = 4 \times 10^{-8}$ cm^3 s^{-1} is higher than the other values of γ even at smaller voltages, as the recombination current is not negligible. Thus, our model can be used to explore the turn on-voltage of QD-LEDs.

IV. CONCLUSION

In this work, we propose a model for QD-LEDs. Our model is able to incorporate the most important parameters that affect the current density and light output of such devices. The device current is mostly limited by the QD layers, where the current is primarily due to recombination of two kinds, radiative and non-radiative. At low voltages, non-radiative recombination dominates the device operation, whereas as the voltage increases, radiative recombination dominates. As the voltage is increased even further, the current is limited by the series resistance of the device, and the current voltage plot becomes essentially linear. There is practically no effect of capture lifetime from the transport layers to the QD layers because the device operation is limited by the QD layers, not how the carriers got into the QDs. Our model is also able to explore the turn-on voltage of QD-LEDs based on the ratio of radiative recombination current to the total device current.

[1]S. Coe, W. K. Woo, and V. B. Moungi Bawendi, Nature **420**(6917), 800 (2002).
[2]M. Schlamp, X. Peng, and A. P. Alivisatos, J. Appl. Phys. **82**, 5837 (1997).
[3]A. H. Mueller, Nano Lett. **5**, 1039 (2005).
[4]B. Kumar, R. Hue, W. L. Gladfelter, and S. A. Campbell, J. Appl. Phys. **112**(3), 034501 (2012).
[5]V. L. Colvin, M. C. Schlamp, and A. P. Alivisatos, Nature **370**, 354 (1994).
[6]S. Coe-Sullivan, J. S. Steckel, W. K. Woo, M. G. Bawendi, and V. Bulovic, Adv. Funct. Mater. **15**, 1117 (2005).
[7]J. Caruge, J. Halpert, V. B. V. Wood, and M. Bawendi, Nat. Photonics **2**(4), 247 (2008).
[8]A. Ekimov and A. Onushchenko, JETP Lett. **34**, 6363 (1981).
[9]D. Weinmann, W. Häusler, and B. Kramer, Phys. Rev. Lett. **74**(6), 984 (1995).
[10]A. Alivisatos, Science **271**(5251), 933 (1996).
[11]S. Gustavsson, R. Leturcq, B. Simovič, R. Schleser, T. Ihn, P. Studerus, K. Ensslin, D. Driscoll, and A. Gossard, Phys. Rev. Lett. **96**, 076605 (2006).
[12]S. M. Cronenwett, T. H. Oosterkamp, and L. P. Kouwenhoven, Science **281**(5376), 540 (1998).
[13]J. Carreras, C. Bonafos, J. Montserrat, C. Domínguez, J. Arbiol, and B. Garrido, Nanotechnology **19**, 205201 (2008).
[14]X. Pi, O. Zalloum, A. Knights, P. Mascher, and P. Simpson, J. Phys.: Condens. Matter **18**, 9943 (2006).
[15]U. Kortshagen, L. Mangolini, and A. Bapat, J. Nanopart. Res. **9**, 39 (2007).
[16]X. Li, Y. He, S. S. Talukdar, and M. T. Swihart, Langmuir **19**(20), 8490 (2003).
[17]J. D. Holmes, K. J. Ziegler, R. C. Doty, L. E. Pell, K. P. Johnston, and B. A. Korgel, J. Am. Chem. Soc. **123**(16), 3743 (2001).
[18]J. Kočka, I. Pelant, and A. Fejfar, J. Non-Cryst. Solids **198**, 857 (1996).
[19]W. Shockley and W. Read, Jr., Phys. Rev. **87**(5), 835 (1952).
[20]R. N. Hall, Phys. Rev. **87**(2), 387 (1952).
[21]R. L. Anderson, Solid-State Electron. **5**(5), 341 (1962).
[22]D. L. Smith, Phys. Status Solidi A **44**(1), 381 (1977).
[23]Y. Liu, C. Gorla, S. Liang, N. Emanetoglu, Y. Lu, H. Shen, and M. Wraback, J. Electron. Mater. **29**, 69 (2000).
[24]H. L. Chen, Y. M. Lu, and W. S. Hwang, Surf. Coat. Technol. **198**(1), 138 (2005).
[25]K. Ellmer, J. Phys. D **34**, 3097 (2001).
[26]R. K. Ligman, L. Mangolini, U. R. Kortshagen, and S. A. Campbell, Appl. Phys. Lett. **90**(6), 061116 (2007).
[27]N. Sobolev, A. Emel'yanov, E. Shek, and V. Vdovin, Physica B **340**, 1031 (2003).
[28]G. Juska, M. Viliunas, K. Arlauskas, and J. Kocka, Phys. Rev. B **51**(23), 16668 (1995).